Galectin-1 in Melanoma Biology and Related Neo-Angiogenesis Processes

Véronique Mathieu[1,9], Elisabeth Martin de Lassalle[2], Jaan Toelen[3], Thomas Mohr[4], Akeila Bellahcène[5], Gwendoline Van Goietsenoven[1], Tina Verschuere[6], Caroline Bouzin[7], Zeger Debyser[3], Steven De Vleeschouwer[6], Stefaan Van Gool[6], Françoise Poirier[8], Vincent Castronovo[5], Robert Kiss[1,9] and Olivier Feron[7]

Aggressiveness of advanced melanomas relates in part to their marked propensity to develop neoangiogenesis and metastases. Among its numerous pro-cancer roles, galectin (gal)-1 expressed and/or secreted by both cancer and endothelial cells stimulates proliferation and angiogenesis. This study first shows that gal-1 is more highly expressed at both mRNA and protein levels than its congeners in melanomas and particularly in advanced lesions. The roles of gal-1 were further investigated *in vivo* in the highly proliferating and vascularized pseudometastatic B16F10 mouse melanoma model using stable knockdown B16F10 cells and wild-type versus gal-1 knockout mice, and then *in vitro* in B16F10 tumoral and lung microvascular cells. Gal-1 depletion in the B16F10 tumor cells but not in the tumor-bearing mice significantly increased melanoma-bearing mice survival. Tumor-derived gal-1 thus seems to have more critical roles than the host-derived one. In fact, gal-1 displays distinct effects on the H-Ras-dependent p53/p21 pathways: in primary lung microvessel endothelial cells, gal-1 seems to be involved in the maintenance of senescent status through the induction of both p53 and p21 while it stimulates B16F10 cancer cell proliferation through a p53/p21 decrease. Altogether, these data point to gal-1 as a potential target to combat melanomas.

Journal of Investigative Dermatology advance online publication, 24 May 2012; doi:10.1038/jid.2012.142

INTRODUCTION

As soon as melanomas have metastasized, they represent one of the most devastating cancer types, with <45% survival 1 year after diagnosis (Balch *et al.*, 2004). This poor prognosis relates mainly (i) to the marked resistance of melanoma cells to pro-apoptotic stimuli and thus to conventional chemotherapy (La Porta, 2009), with clinical response rates that do not exceed 15–20% (Mouawad *et al.*, 2010), and (ii) to the ability of melanoma cells to escape from natural, endogenous, or therapeutically induced immune attacks (Gajewski, 2007). Hypoxia favors melanoma progression (Bedogni and Powell, 2009), and melanomas are associated with marked neoangiogenesis processes. Therefore, great hopes have been placed in anti-angiogenic therapies to combat advanced melanomas (Mansfield and Markovic, 2009; Marneros, 2009).

Galectin-1 (gal-1) belongs to a family of 15 β-galactoside-binding proteins in mammals sharing a consensus carbohydrate recognition domain of 135 amino acids (Barondes *et al.*, 1994; Camby *et al.*, 2006). Gal-1 and gal-3 are hypoxia-regulated proteins (Greijer *et al.*, 2005; Le *et al.*, 2005) that exert important roles in neoangiogenesis processes (Thijssen *et al.*, 2006, 2008, 2010).

Gal-1, -3, and -9 have been shown to participate in the regulation of the tumor immune response (Rubinstein *et al.*, 2004; Liu and Rabinovich, 2010), adhesion, migration, and metastasis (Danguy *et al.*, 2002; Camby *et al.*, 2006; Elola *et al.*, 2007); gal-1 and -3 participate in transformation and proliferation (Paz *et al.*, 2001; Elad-Sfadia *et al.*, 2002, 2004), apoptosis, and chemoresistance (Fukumori *et al.*, 2007; Le Mercier *et al.*, 2008a); and gal-1 participates in stem cell differentiation (Nasrabadi *et al.*, 2010).

In melanoma cells, the expression of gal-1 and -3 *in vitro* was first reported in 1989 (Lotan *et al.*, 1989). Although data regarding the potential roles of gal-1 in melanomas are much

[1]*Laboratoire de Toxicologie, Faculté de Pharmacie, Université Libre de Bruxelles (ULB), Brussels, Belgium;* [2]*Institut de Pathologie, Pôle de Biologie, Pathologie et Génétique du CHRU de Lille, Lille, France;* [3]*Laboratory for Molecular Virology and Gene Therapy, University Hospital Gasthuisberg, Catholic University Leuven, Leuven, Belgium;* [4]*Department of Medicine I, Institute of Cancer Research, Medical University of Vienna, Vienna, Austria;* [5]*Metastasis Research Laboratory, GIGA Cancer, Liège University, Liège, Belgium;* [6]*Laboratory of Experimental Immunology, University Hospital Gasthuisberg, Catholic University Leuven, Leuven, Belgium;* [7]*Angiogenesis and Cancer Research Laboratory, Pole of Pharmacology and Therapeutics, Institut de Recherche Expérimentale et Clinique (IREC), Université Catholique de Louvain (UCL), Brussels, Belgium and* [8]*Institut Jacques Monod, UMR 7592 CNRS, Université Paris Diderot, Paris, France*

[9]*VM is a Post-Doctoral Fellow and R.K. a Director of Research with the Fonds National de la Recherche Scientifique (FNRS, Belgium).*

Correspondence: Veronique Mathieu, Laboratory of Toxicology, Faculty of Pharmacy, Free University of Brussels (ULB), Campus de la Plaine, Boulevard du Triomphe, 1050 Brussels, Belgium. E-mail: vemathie@ulb.ac.be

Abbreviations: gal-1, galectin; KD, knockdown; LMECs, lung microvessel endothelial cells; ROS, reactive oxygen species

Received 12 September 2011; revised 13 February 2012; accepted 1 March 2012

more limited than for gal-3 to date, we were nevertheless the first to suggest a gal-1-mediated modulation of melanoma cell adhesion to laminin (van den Brûle *et al.*, 1995). Gal-1 and -3 are both associated with metastatic development in experimental melanomas metastazing to the lungs (Rye *et al.*, 1998). *In vivo* administration of carbohydrate recognition domain competitors decreases lung colonization by melanoma cells (Platt et Raz, 1992; Krishnan *et al.*, 2005).

Considering the multifaceted roles of gal-1 reported above with respect to cancer cell, as well as endothelial cell biology, this study aims (i) to compare its expression level with other galectins in benign *nevi* and melanoma progression and (ii) to further decipher mechanistically its differential roles in cancer versus endothelial cell biology in the specific lung context.

RESULTS

Gal-1 is more highly expressed than gal-3 and -9 in melanomas

Figure 1a–c illustrate the mRNA expression levels of gal-1, -3, and -9, respectively, in a public Affymetrix data set relating to samples from human normal skin ($n=7$), benign nevi ($n=18$), and melanomas ($n=45$). Although gal-9 mRNA expression remains low in the three groups, gal-1 and -3 mRNAs are significantly higher in melanoma samples as compared with normal or benign tissues. The mRNA expression levels of the remaining galectins, i.e., gal-2, -4, -7, -8, -13, and -14 were found in low amounts in all groups except for gal-7 in the benign nevi group (data not shown).

The cellular effects of galectins can markedly vary in function of their localizations (Califice *et al.*, 2004). We thus investigated gal-1,-3, and -9 cytoplasmic versus nuclear protein expression by immunohistochemistry in a clinical series of 57 benign *nevi* and 82 melanomas. Quantification of the cytoplasmic versus nuclear (Table 1) gal staining according to the Breslow index shows that (i) gal-1 is the highest expressed gal as compared with gal-3 and gal-9 in both cellular compartments, (ii) gal-1 is more highly expressed in the cytoplasm of advanced melanoma lesions as compared with gal-3 and -9, and (iii) gal-9 is poorly expressed in all lesions as illustrated by examples in Figure 1f–n. Staining intensity was higher for gal-1 than for gal-3 in advanced melanoma lesions (b3, b4, and MM) while being very low for gal-9 (Table 1).

Gal-1 depletion extends survival of melanoma-bearing mice

To further examine a possible role of gal-1 in the metastatic progression of melanoma, we evaluated the impact of its downregulation in the B16F10 mouse melanoma model. Among the 30 stable gal-1 knockdown (KD) B16F10 clones that were engineered in the current study, the highest decrease (~80%) in gal-1 expression was obtained in clone 1.3 (Figure 2a), which was selected for all subsequent studies and further named KD.

Gal-1 KD versus mock and wild-type B16F10 cells were grafted intravenously (tail vein) in immunocompetent mice. Wild-type B16F10 melanoma cells formed aggressive lung

Table 1. Clinical data of galectins' staining

		Nevi	B1	B2	B3	B4	MM
	N	57	18	8	8	10	38
Cytoplasmic							
Gal-1	++/+++ (%)	93	82*	86*	57*	70	82
	AREA (%)	61	62*	67*	73*	70	50
Gal-3	++/+++ (%)	98*	81**	86*	88	80	84
	AREA (%)	53*	50**	63*	34	33	32
Gal-9	++/+++ (%)	35***	33	78	86*	70	61
	AREA (%)	31***	17	23	21*	22	18
Nuclear							
Gal-1	++/+++ (%)	72	65*	71*	43*	100 Weak	61
	AREA (%)	50	53*	66*	49*	79	40
Gal-3	++/+++ (%)	48*	31**	72*	50	100 Weak	63
	AREA (%)	37*	36**	44*	36	43	24
Gal-9	++/+++ (%)	44***	33	88	86*	70	63
	AREA (%)	21***	15	22	21*	16	15
Global							
Gal-1	++/+++ (%)	91	82*	86*	57*	70	79
	AREA (%)	72	64*	67*	73*	70	63
Gal-3	++/+++ (%)	88	56**	71*	63	20*	51*
	AREA (%)	71	66**	69*	69	67*	60*
Gal-9	++/+++ (%)	39***	28	88	71*	50	55
	AREA (%)	31***	17	28	31*	29	21

Abbreviation: gal, galectin.
Each star (*) indicates that one clinical slide was missing within the group regarding the gal studied. Only the percentage of strong intensities (++/+++) is mentioned with the exception of the nuclear gal-1 and gal-3 staining in group B3, for which the staining intensity was weak in all cases but in a large proportion of cells.
The groups B1–B4 relate to primary melanomas with Breslow index categories 1–4; 1: Breslow <1 mm; 2: Breslow between 1 and 2 mm; 3: Breslow between 2 and 4 mm; 4: Breslow >4 mm. MM relates to metastatic melanomas.

Figure 1. Galectin (gal)-1, -3, and -9 expression levels in tumor progression. The mRNA expression levels of (**a**) gal-1, (**b**) gal-3, and (**c**) gal-9 in the public Affymetrix array data set GSE3189 (new genes associated with malignant melanoma but not benign melanocytic lesions) of normal skin samples (NS; $n=7$), benign *nevi* (BN; $n=18$), and malignant melanomas (MM; $n=45$). Data are expressed as mean ± SEM and *** relates to *P*-value <0.001. (**d**) Typical cytoplasmic and (**e**) nuclear strong staining (++/+++; GX400). Typical staining patterns of (**f**) gal-1, (**g**) gal-3, and (**h**) gal-9 in a human benign composed *nevus*, (**i–k**) the ones of a Dubreuil melanoma sample of Breslow index 4 (>4 mm; GX400) and (**l–n**) the ones of a brain metastatic melanoma lesion. Gal immunostaining appears red, and slides have been counter-colored with hematoxylin–eosin. a.u., arbitrary units. Bar = 50 μm.

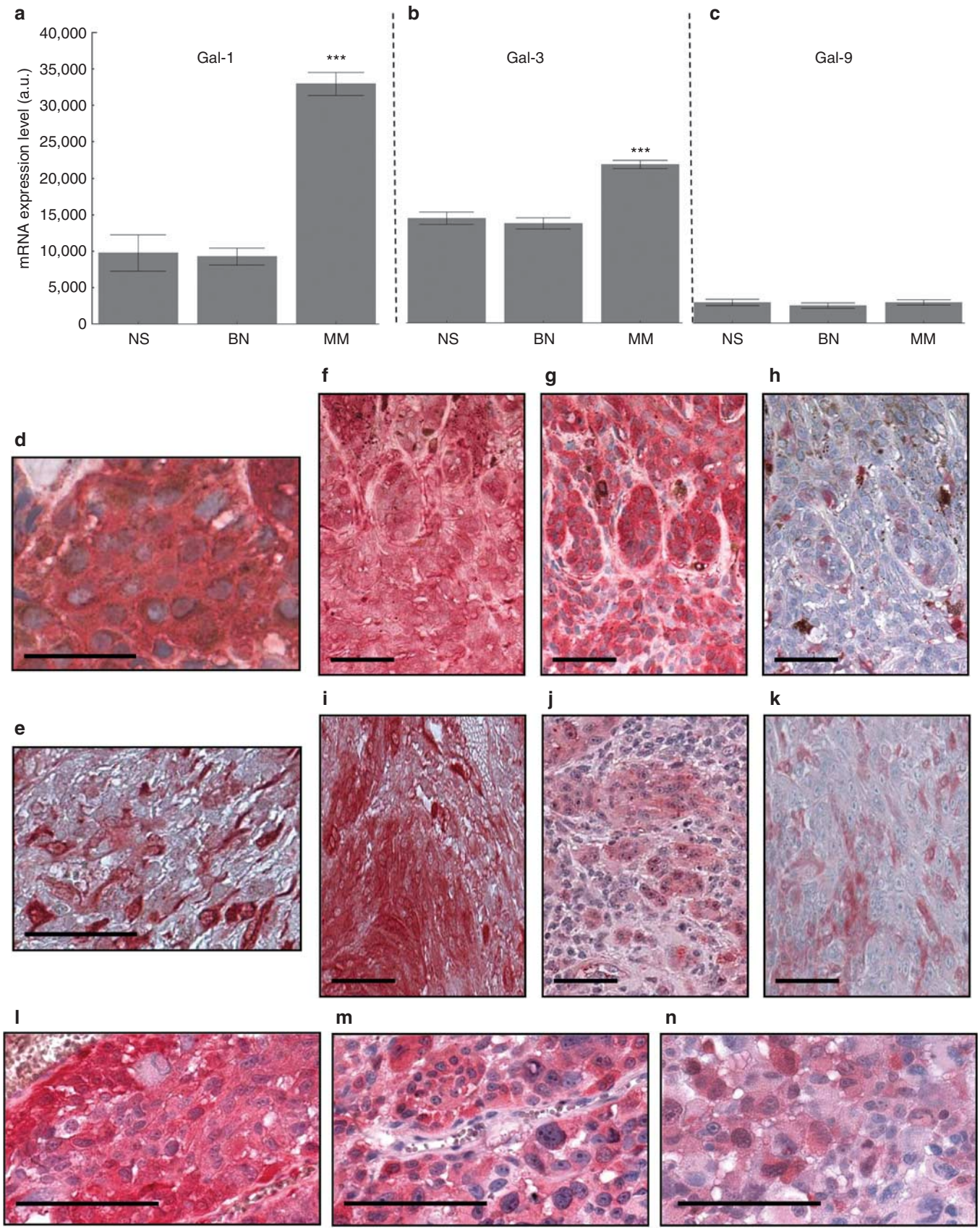
a
b
c
Gal-1
Gal-3
Gal-9
***
***
mRNA expression level (a.u.)
40,000
35,000
30,000
25,000
20,000
15,000
10,000
5,000
0
NS
BN
MM
NS
BN
MM
NS
BN
MM
d
e
f
g
h
i
j
k
l
m
n

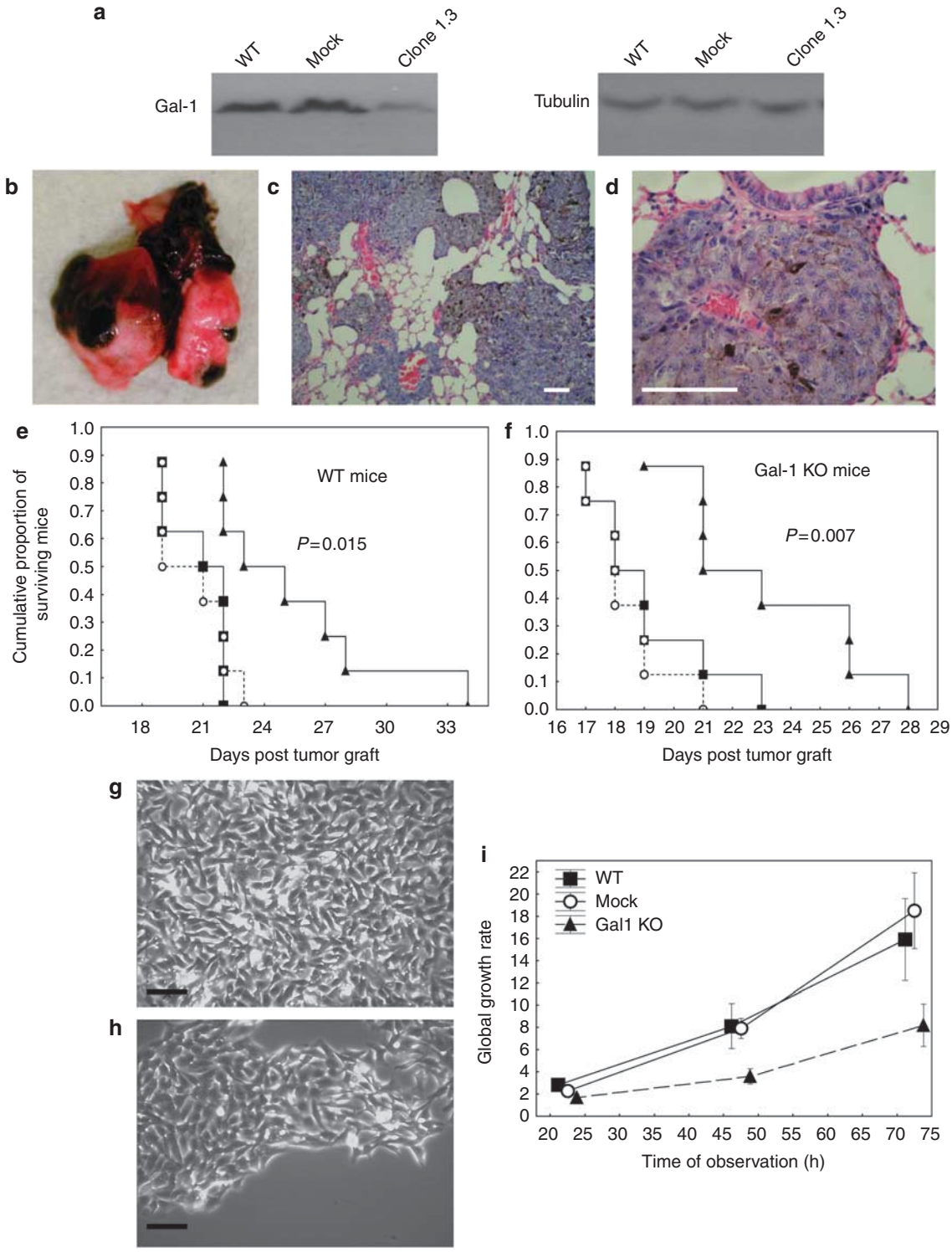

Figure 2. Galectin (gal)-1-deficient mouse melanoma models display increased survival. (**a**) Western blot analysis of gal-1 expression levels in wild-type (WT), mock-transfected, and monoclonal (clone 1.3) gal-1 knockdown (KD) B16F10 melanoma cell lines; 20 μg of protein was loaded for each sample. Integrity of the samples was assessed by tubulin immunoblotting. (**b**) This picture illustrates the macroscopic tumor that developed in the lungs of immunocompetent mice that were grafted in the tail vein with murine B16F10 melanoma cells. Hematoxylin–eosin (HE) staining pictures at (**c**) GX100 and (**d**) GX400 of the tumor that developed in the lung parenchyma. Bar = 100 μm. (**e**) This graph presents the Kaplan–Meier survival curves of mice (eight mice per experimental group) grafted with wild-type versus gal-1-deficient melanoma cells into their tail veins (black squares: wild-type group; open dots: mock transfected group; black triangles: clone 1.3). (**f**) A similar survival curve was drawn when the same cell subtypes were grafted in gal-1 knockout (KO) mice. Same legend. Videomicroscopic pictures after 72 hours of observation of (**g**) wild-type and (**h**) gal-1-KD B16F10 melanoma cells. Bar = 100 μm. (**i**) Quantification of the number of cells over time shows that gal-1 depletion markedly reduces cell proliferation.

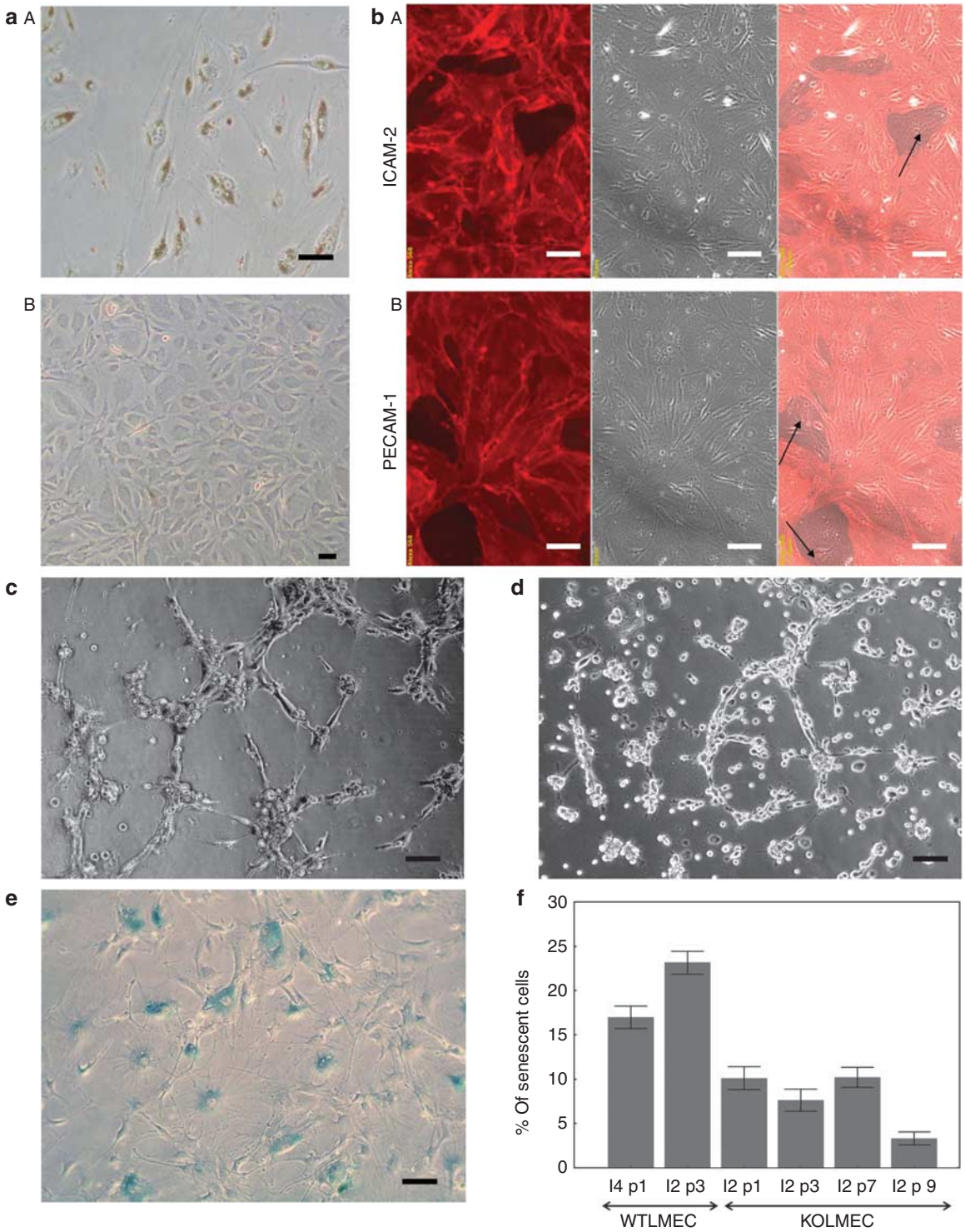

Figure 3. Galectin-1-deficient endothelial cell properties. (**a**) Isolation of primary lung mouse endothelial cells (LMEC) with (**a**A) Dynabeads and (**a**B) typical endothelial morphology obtained after the second marker selection (passage 1). (**b**) Immunofluorescence staining of WTLMECs for PECAM-1 and ICAM-2 after the primary isolation with anti-PECAM-1 antibody. Arrows on the merged pictures point to the rare unstained cells (<5% of the whole population) before the second sorting. Similar results were obtained for KOLMEC (data not shown). (**c**, **d**) The ability of the LMEC to form a tubular network when cultured on Matrigel: whereas (**c**) WTLMECs form such networks 3 hours after the seeding, (**d**) KOLMECs cannot. Observation was continued for 48 hours without any success. (**e**) WTLMECs became senescent after three passages with the active beta-galactosidase stained in blue. Quantification of the percentage of beta-galactosidase-positive cells over the passages is presented in **f**. Data are presented as mean ± SEM of 10 fields per flask; IxPy: x and y relate to the isolation assay and cell culture passage numbers, respectively. Bar = 100 μm.

tumors (pseudometastases) as observed 3 weeks after their injection (Figure 2b–d).

Survival analysis shows that gal-1-competent mice grafted with gal-1 KD B16F10 cells survived significantly longer than the control groups ($P = 0.015$; Figure 2e). Similar results were obtained when the B16F10 melanoma cell subtypes (wild type, mock, and KD) were grafted in gal-1-deficient (knockout) mice (Figure 2f). The lack of differences between data obtained in gal-1-competent (Figure 2e) versus gal-1 knockout mice (Figure 2f) suggest that the aggressiveness of the intravenous B16F10 melanoma model relates mainly to the B16F10 cell-related content in gal-1 and not to the host (mice) content in gal-1. We recently showed that gal-1-deficient endothelial cells can take up the tumor-secreted gal-1 for angiogenesis (Thijssen *et al.*, 2010). As gal-mediated interactions between cancer cells and microvessel endothelial cells have important roles in melanoma metastases and progression (Platt et Raz, 1992; Rye *et al.*, 1998; Krishnan *et al.*, 2005), we further investigated gal-1-mediated effects and signaling pathways not only in B16F10 melanoma cells but also in primary lung endothelial cells as detailed below.

Gal-1 depletion modifies the growth properties of melanoma cells *in vitro*

Although control B16F10 cells rapidly reached confluency after subculture, gal-1 depletion markedly decreased the global growth rate of B16F10 cells (Figure 2g–i).

Gal-1 depletion impairs angiogenic properties of endothelial cells but rescues primary endothelial cells from early cell cycle arrest

As illustrated above, B16F10 melanoma cells home in the lungs after intravenous injection and thus need to interact with lung microvessel endothelial cells (LMECs). To study the possible influence of gal-1 on the vascular compartment of metastases, we isolated LMECs from wild-type (WTLMECs) versus gal-1 knockout mice (KOLMECs) by two consecutive sortings with magnetic Dynabeads coated with PECAM-1 and ICAM-2 LMEC cell markers, respectively (Figure 3aA). Isolated LMECs exhibited typical endothelial cell morphology (Figure 3aB); purity of the cell populations was assessed by immunofluorescence for both PECAM-1 and ICAM-2 markers as illustrated in Figure 3bA and bB.

When cultured on Matrigel, the WTLMECs form tubular networks (Figure 3c) to a larger extent than KOLMECs (Figure 3d), which is in accordance with previous published results that demonstrated the roles of gal-1 in neoangiogenesis (Thijssen *et al.*, 2006, 2008, 2010).

Among five independent WTLMEC cell isolation assays, only three succeeded in obtaining growing cell culture until passages three to four, whereas the two unsuccessful assays could not reach passage one. By contrast, KOLMEC cells were proliferating until at least passage nine in two of the four experimental isolations performed. Determination of β-galactosidase activity revealed that at least 25% of WTLMECs were senescent at passage three (Figure 3e and f), whereas the proportion of senescent cells in KOLMECs remained $<10\%$ over the passages (at least until passage nine; Figure 3f).

Gal-1-related effects on cell growth depend on the p53/p21 pathway that can be triggered by Ras

Senescence in normal cells such as fibroblasts was shown previously to depend on Ras signaling. Ras can actually trigger proliferation signals in malignant cells and senescence in primary fibroblast cell cultures (Benanti and Galloway, 2004). Considering the fact that gal-1 has a critical role in the plasma membrane anchorage of H-Ras and its subsequent signaling (Paz *et al.*, 2001; Elad-Sfadia *et al.*, 2002; Belanis *et al.*, 2008), we hypothesized that gal-1 depletion could lead to opposite consequences in B16F10 melanoma cells and ''healthy'' LMECs. Indeed, although gal-1 KD induces a marked increase in p53 expression level in melanoma cells, (Figure 4a) as previously reported in the case of glioma cells (Camby *et al.*, 2005), KOLMECs display a lower level of this protein as compared with WTLMECs (Figure 4b). This observation was confirmed by immunofluorescence: although p53 and its downstream target p21 are overexpressed in gal-1 KD B16F10 melanoma cells (Figure 4c), their expression levels are markedly decreased in KOLMECs as compared with WTLMECs (Figure 4d). Other important controllers of the cell cycle and the induction of senescence, i.e., p16 and Rb, have also been investigated but were not expressed at detectable levels in our samples (Figure 4a and b). Although the total level of Ras does not seem to be altered by gal-1 depletion (Figure 4a and b), its expression pattern and distribution could be modified when comparing gal-1-expressing versus gal-1-depleted cells as presently revealed by optical sections in the case of LMECs: plasma membrane–associated Ras appears more marked in KOLMECs than in the WTLMECs (Figure 4d).

DISCUSSION

Gal-1 is expressed in a large set of human tumor types (Danguy *et al.*, 2002; Liu and Rabinovich, 2005; Demydenko and Berest, 2009). Although major attention has been paid to gal-3 and -9 in melanomas, the current study indicates that gal-1 is more highly expressed in advanced melanoma lesions than the other galectins. We accordingly show here that stable gal-1 depletion in B16F10 melanoma cells reduces their proliferation rate *in vitro* and thereby partly increases the survival of mice grafted with those cells (vs. wild-type B16F10 cell administration). Our data further revealed that gal-1 depletion in host mice (i.e., gal-1 KO mice) did not contribute higher benefits in terms of survival, indicating that the melanoma cell contribution to the gal-1 pool of the lung metastases is more critical than that of the host. In addition to the capacity of endothelial cells to take up the tumor-secreted gal-1 to stimulate neoangiogenesis (Thijssen *et al.*, 2010), compensatory mechanisms may have been activated in knockout mice but not *in vitro* in melanoma cells. Nevertheless, a similar phenomenon was also observed in the case of gal-3 KO mice (Thijssen *et al.*, 2008; Eude-Le Parco *et al.*, 2009). Interestingly, besides the confirmation of the pro-angiogenic role of gal-1, our data identified a role of gal-1 in the regulation of cell senescence. In particular, we documented the gal-1-dependent senescence of the cells located at the interface between circulating B16F10 melanoma cells

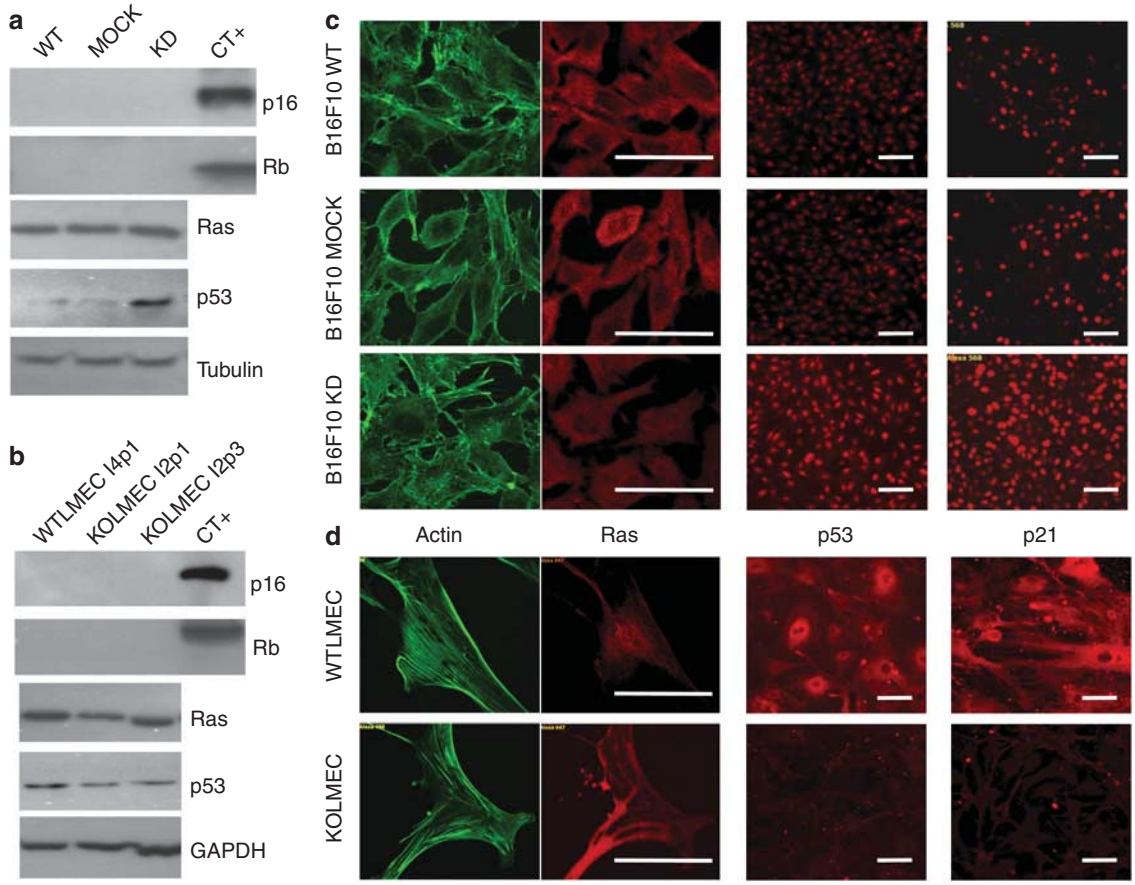

Figure 4. Identification of the molecular pathways involved in galectin (gal)-1-dependent modifications of the growth properties of melanoma cells and lung microvessel endothelial cells (LMECs). (**a**) Protein expression levels of Ras, p53, p16, and Rb in B16F10 melanoma cells assessed by western blot. (**b**) Protein expression levels of the same proteins in WTLMECs versus KOLMECs at various passages. Immunofluorescence staining for Ras, p53, and p21 in (**c**) mouse melanoma cells and (**d**) LMECs. Ras expression was evaluated by pseudo-confocal fluorescent microscopy at GX40, with focus on fibrillar actin staining represented in green. In the case of LMECs, illustrations are provided for I5P2 and I4P4 in WTLMECs and KOLMECs, respectively; p53 and p21 of WTLMEC and KOLMEC staining are illustrated for the I1P3 and I2P7, respectively (GX10; nonconfocal microscopy). KD, knockdown; KO, knockout; WT, wild type. Bar = 100 μm.

and the host lung tissues, namely the lung microvascular endothelial cells.

The present study shows that gal-1 depletion decreases the proliferation of melanoma cells, whereas it rescues primary lung mouse endothelial cells from early cell cycle arrest. To understand the opposite roles of gal-1 on melanoma and lung microvascular endothelial cells, we examined the influence of gal-1 downregulation on the expression of Ras and p53, two key regulators of cell survival and senescence, further noting that gal-1 was previously reported to be a key partner of Ras: gal-1 is required to anchor the active farnesylated form of Ras at the plasma membrane (Paz *et al.*, 2001; Belanis *et al.*, 2008) and leads to the stimulation of cancer cell proliferation and survival (Schubbert *et al.*, 2007). The decrease in melanoma cell proliferation observed in gal-1 KD B16F10 cells could result from the impairment of Ras activity. In gal-1 KD B16F10 cells, we also identified a marked increase of both p53 and p21 expression levels (vs. wild-type B16F10 cells). These data support a decreased apoptotic potential of gal-1-expressing tumor cells; such link between gal-1 expression and p53 induction was already observed in glioma cells (Camby *et al.*, 2005). In contrast, lack of gal-1 in LMECs was associated with a reduced expression of p53 and p21, which was in accordance with a reduced or delayed senescence. Normal cells have been shown to either senesce or transform in response to H-Ras-induced expression in a cellular status– and context-dependent manner (Benanti and Galloway, 2004). Ras family members' oncogenic roles in cancer cell proliferation and survival are largely documented (Schubbert *et al.*, 2007). However, transduced expression of H-Ras in normal fibroblasts or keratinocytes can induce their senescence (Serrano *et al.*, 1997; Lin and Lowe, 2001). Two major pathways have been identified in this process: p16/Rb and p53/p21 through or not through Rb, although their respective roles remain controversial (Serrano *et al.*, 1997; Benanti and Galloway, 2004; Yaswen and Campisi, 2007). In fact, the requirements for maintaining senescence arrest are less well known than the requirements to establish it. Replicative senescence can be reversed by p53 inactivation, but only in p16-negative cells (Beauséjour *et al.*, 2003).

Therefore, p16 seems to be a dominant irreversible barrier to cell proliferation (Beauséjour *et al.*, 2003). Here we show that gal-1 KOLMEC cells exhibit decreased expression levels of both p53 and p21, both WTLMEC and KOLMEC cells being p16 and Rb negative. These results therefore completely fit with the senescence reversal pathway published previously in the case of fibroblasts (Beauséjour *et al.*, 2003). Moreover, endothelial cell senescence has been later related to inhibition of the CDK2 activity that results from both a reduced CDK2 expression level and CDK2 inhibition by p21 but is independent of p16 (Freedman and Folkman, 2005).

Finally, p53- but not p16-dependent cell senescence has been linked to the production of reactive oxygen species (ROS), notably in the context of normal endothelial cells (Cho *et al.*, 2011), whereas tumor aggressiveness and neoangiogenesis can be both increased by Akt and/or NOX-1-induced ROS (Arbiser *et al.*, 2002; Govindarajan *et al.*, 2007). Therefore, ROS could be key mediators of the gal-1 opposite cell cycle regulation in cancer versus endothelial cells observed in the present study, especially when considering that galectins' expression or signaling has been associated with ROS production (Mendelsohn *et al.*, 2007; Zhuravliova *et al.*, 2009).

Our study therefore emphasizes gal-1 as a key target to combat cancer progression, by acting not only on tumor cells but also on host endothelial cells. First, our data confirm the anti-angiogenic potential of blocking gal-1 effects as previously demonstrated with the anginex anti-angiogenic peptide whose activity depends on direct gal-1 binding (Thijssen *et al.*, 2006). Second, our study provides evidence for a direct link between gal-1 and the senescence of lung microvascular endothelial cells. Blocking the effects of gal-1 may reduce the homing of circulating tumor cells and thereby decrease metastatic spreading. Interestingly, salirasib, a compound in phase II clinical trial evaluation designed to inhibit H-Ras signaling was shown to compete for the gal-1 binding site with farnesylated H-Ras (Paz *et al.*, 2001). Considering the fact that salirasib preferentially inhibits the plasma membrane anchorage of the active H-Ras 12V form in comparison with the wild-type form, such compounds could differentially act on the oncogenic versus senescent H-Ras pathways. In addition to anginex and salirasib, the silencing of gal-1 using dedicated siRNA could also be used to combat melanomas. We already demonstrated *in vivo* the feasibility of such an approach not only in experimental melanomas (Mathieu *et al.*, 2007) but also in experimental gliomas (Le Mercier *et al.*, 2008b).

In conclusion, our study has documented that the highly expressed gal-1 in aggressive melanoma actively participates in the metastatic progression of the disease. Besides the already well-documented pro-angiogenic and trophic effects of gal-1, our study unravels a role of gal-1 in the senescence of lung microvascular endothelial cells at the metastatic site. This process is supported by a distinct capacity of melanoma cells and host endothelial cells to stimulate the p53/p21 pathway that could depend on Ras. More generally, this study gives more credential to strategies such as anginex, salirasib, and anti-gal-1 siRNA, aiming to interfere with gal-1 functions in cancers and, in particular, in melanoma.

MATERIALS AND METHODS

Antibodies

All antibodies used in the present study are detailed in the Supplementary Information online.

Cell cultures

B16F10 mouse melanoma cells (ATCC code CRL-6475) were purchased from the ATTC (Manassas, VA) and cultured as previously described (Mathieu *et al.*, 2007).

Construction of gal-1-depleted B16F10 mouse melanoma cells

Stable KD cells were generated using HIV-based vectors encoding the miRNA-based short-hairpin RNAs against gal-1 with a blasticidin resistance cassette; 30 monoclonal gal-1 KD cell lines were generated. Selection of the best clones was based on their gal-1 expression level as determined by western blot analysis. The detailed procedure is described in the SI section.

Quantitative videomicroscopy

Computer-assisted phase contrast microscopy (quantitative videomicroscopy) enabled us to follow and quantify the growth rates and behavior of B16F10 melanoma cell subtypes over a 72-hour period, as detailed in Debeir *et al.* (2008).

Primary endothelial cell isolation and culture

Lung mouse endothelial cells (LMECs) were isolated as described by Lim *et al.* (2003). Briefly, lungs from three mice were collected, minced, and digested in collagenase IV (Worthington, Gestimed, Brussels, Belgium) for 1 hour at 37 °C under agitation. After filtration (40 μm BD filter), cells were centrifuged and incubated with Dynabeads coated with anti-PECAM-1 antibody (BD Pharmingen, Erembodegem, Belgium) at room temperature for 30–60 minutes under agitation. After magnetic separation and three washing steps, cells were allowed to adhere and grow in a 25-cm^2 flask coated with fibronectin (2.5 μg cm^{-2}, Millipore, Brussels, Belgium). When cells reached confluence, they were detached with trypsin-EDTA (Invitrogen, Merelbeek, Belgium) for their first passage, centrifuged, and sorted again with Dynabeads coated with anti-ICAM-2 antibody (BD Pharmingen) as detailed above. The detailed procedure and product references are available at http://vrd.bwh.harvard.edu/core_facilities/mlec.html.

Five (wild-type mice) and four (gal-1 KO C57Bl/6 mice) distinct isolations have been performed (see *in vivo* experiments).

Tubulogenesis

For the tubulogenesis assay, 100,000 endothelial cells were seeded in 500-μl endothelial growth medium on pure Matrigel (BD Biosciences, Erembodegem, Belgium) matrix in 24-well plates. Pictures of the network formed were taken 3 hours after the seeding. We followed this for 48 hours after the seeding to monitor for late development. The experiment was conducted in triplicate.

Senescence assay

Senescent cells display increased beta-galactosidase levels (Itahana *et al.*, 2007). Therefore, beta-galactosidase activity measurement was conducted with the colorimetric Senescence Detection Kit (Sigma-Aldrich, Bornem, Belgium) following the manufacturer's recommendations. X-gal is an organic compound of galactose linked to a substituted indole that is cleaved by β-galactosidase, yielding galactose and 5-bromo-4-chloro-3-hydroxyindole. The latter is then

oxidized into 5,5′-dibromo-4,4′-dichloro-indigo, an insoluble blue product. The lung mouse endothelial cells were evaluated after each passage 3–5 days following seeding in 12.5-cm^2 flasks. Ten fields (GX10) per flask were quantified for the proportion of beta-galactosidase-positive cells.

Protein expression pattern evaluation

Western blot. Gal-1 expression level in the various monoclonal melanoma cells was evaluated by means of western blot analysis as previously described (Mathieu *et al.*, 2007). The integrity and equal loading of the extracts were evaluated by tubulin or GAPDH blot. Quantification of the signal was determined using the Aida Software and has been normalized against the background.

Immunofluorescence. For immunofluorescence staining, cells were cultivated on glass coverslips for 48–72 hours and fixed with 3.5% formalin in phosphate-buffered saline for 20 minutes at 4 °C. Cells were permeabilized with 0.2% Triton X-100 for 10 minutes at room temperature when required. Antibodies and dilutions are provided in the SI section. Images were collected with a Zeiss Axio microscope (Zeiss, Zaventem, Belgium).

Fluorescence assays on LMECs have been performed on the fixed materials for the beta-galactosidase staining. The fixative solution is a mixture of formaldehyde and glutaraldehyde (Sigma-Aldrich, Senescence Detection Kit). Therefore, the aldehyde groups that could lead to nonspecific staining were reduced with $NaBH_4$ in phosphate-buffered saline (0.5 mg ml^{-1}), pH 8.0, for 10 minutes and repeated three times after a short permeabilization in 100% ice-cold methanol (10 seconds) before the staining procedure described above.

Ras imaging microscopy was realized on plastic coverslips fixed with a mixture of formaldehyde and glutaraldehyde (Sigma-Aldrich, Senescence Detection Kit) and permeabilized with 0.2% Triton $\times$100 for 10 minutes. Nonspecific reaction and/or binding were avoided by incubation with 1% FBS in phosphate-buffered saline for 30 minutes before staining. Plasma membrane was visualized by Alexa Fluor 488–coupled phalloidin (Molecular Probes, Invitrogen). Optical sectioning was obtained by structured illumination using an Apotome system (Zeiss) coupled to an AxioImager microscope (Zeiss) and analyzed using the dedicated AxioVision software (Zeiss).

Microarray data management

We analyzed the mRNA expression levels of galectins in the public data set GSE3189 (GPL96 platform, GEO DataSets, PubMed database). It was obtained with the Affymetrix Human Genome U133A Array (Affymetrix, Santa Clara, CA). mRNA expression data are presented in the database as normalized values in arbitrary units and are therefore ready to use. All gal data were selected for further analysis. Gal-2, -3, -4, -7, -9, -13, and -14 were represented on the array by one oligo, gal-1 by two oligos, and gal-8 by six oligos. The data set contains 7 normal skin samples, 18 benign *nevi*, and 45 melanomas. Expression level of gal varied from 5 to 55, 563 arbitrary units. Comparison between the groups has been made both separately on each oligo and on their mean in case of multiple oligos. For gal-1, among the two oligos of the array, we present here only the data for one of them, because the second one displayed values around 100 arbitrary units. However, its significant increased expression level in metastatic lesions was obtained with both oligos.

Immunohistological staining

Immunohistochemical expression of gal-1, -3, and -9 was determined on a series of 139 clinical samples including 57 *nevi* and 82 melanomas (Table 1). Samples were obtained from the Pôle de Biologie, Pathologie et Génétique (CHRU Lille Hospital, France), and the Erasmus University Hospital (Brussels, Belgium). Four consecutive 5-μm slides were used for each case for one hematoxylin–eosin and the three gal stainings. The semiquantitative analysis was performed by a specialized pathologist and assessed global, cytoplasmic, and nuclear expressions (Figure 1d and e) in terms of the percentage of cells stained and the intensity of staining (0/+ vs. ++/+++, see Figure 1k and g or i respectively).

In vivo experiments

Five-hundred thousand mouse melanoma cells were injected intravenously in the tail vein of the mice. Wild-type 6-week-old C57BL/6 mice were purchased from Charles Rivers (Arbresle, France). Knockout mice have been generated and bred in our lab (Poirier and Robertson, 1993). Each group contained eight mice.

The *in vivo* experiment described in the present study was conducted on the basis of Authorization No. LA1230568 of the Animal Ethics Committee of the Federal Department of Health, Nutritional Safety and the Environment (Belgium).

Statistical analysis

Statistical comparisons between groups were established by carrying out the Kruskal–Wallis test. Survival analyses were carried out by means of Kaplan–Meier curves and log-rank tests. All statistical analyses were performed using Statistica (Statsoft, Tulsa, OK).

CONFLICT OF INTEREST

The authors state no conflict of interest.

ACKNOWLEDGMENTS

The present work has been supported partly by grants awarded by the Fonds Yvonne Boël (Brussels; Belgium) and by the FNRS (Brussels, Belgium).

Author Contributions

VM, OF, and RK originally initiated the project. Clinical series, staining, and analyses were performed by EMD, AB, and VC. VM, GVG, TM, and JT with TV carried out the experiments under the direction and supervision of their mentors, i.e., OF (for VM) and RK (VM and GVG), ZD, SDV, and SVG (for JT and TV). FP provided gal-1 KO mice breading for all *in vivo* experiments and isolation of microvessel endothelial cells. CB and VM performed the pseudoconfocal experiment. VM, OF, and RK wrote the manuscript. All authors provided constructive criticism and review of the paper. All authors approved the paper in its present form before submission.

SUPPLEMENTARY MATERIAL

Supplementary material is linked to the online version of the paper at http://www.nature.com/jid

REFERENCES

Arbiser JL, Petros J, Klafter R *et al.* (2002) Reactive oxygen generated by Nox1 triggers the angiogenic switch. *Proc Natl Acad Sci USA* 99:715–20

Balch CM, Soong SJ, Atkins MB *et al.* (2004) An evidence-based staging system for cutaneous melanoma. *CA Cancer J Clin* 54:131–49

Barondes SH, Castronovo V, Cooper DN *et al.* (1994) Galectins: a family of animal beta-galactoside-binding lectins. *Cell* 76:597–8

Beauséjour CM, Krtolica A, Galimi F *et al.* (2003) Reversal of human cellular senescence: roles of the p53 and p16 pathways. *EMBO J* 22:4212–22

Bedogni B, Powell MB (2009) Hypoxia, melanocytes and melanoma – survival and tumor development in the permissive microenvironment of the skin. *Pigment Cell Melanoma Res* 22:166–74

Belanis L, Plowman SJ, Rotblat B *et al.* (2008) Galectin-1 is a novel structural component and a major regulator of h-ras nanoclusters. *Mol Biol Cell* 19:1404–14

Benanti JA, Galloway DA (2004) The normal response to RAS: senescence or transformation? *Cell Cycle* 3:715–7

Califice S, Castronovo V, Bracke M *et al.* (2004) Dual activities of galectin-3 in human prostate cancer: tumor suppression of nuclear galectin-3 vs tumor promotion of cytoplasmic galectin-3. *Oncogene* 23:7527–36

Camby I, Decaestecker C, Lefranc F *et al.* (2005) Galectin-1 knocking down in human U87 glioblastoma cells alters their gene expression pattern. *Biochem Biophys Res Commun* 335:27–35

Camby I, Le Mercier M, Lefranc F *et al.* (2006) Galectin-1: a small protein with major functions. *Glycobiology* 16:137R–57R

Cho JH, Kim MJ, Kim KJ *et al.* (2011) POZ/BTB and AT-hook-containing zinc finger protein 1 (PATZ1) inhibits endothelial cell senescence through a p53 dependent pathway. *Cell Death Differ* 19:703–12

Danguy A, Camby I, Kiss R (2002) Galectins and cancer. *Biochim Biophys Acta* 1572:285–93

Debeir O, Mégalizzi V, Warzée N *et al.* (2008) Videomicroscopic extraction of specific information on cell proliferation and migration *in vitro*. *Exp Cell Res* 314:2985–98

Demydenko D, Berest I (2009) Expression of galectin-1 in malignant tumors. *Exp Oncol* 31:74–9

Elad-Sfadia G, Haklai R, Balan E *et al.* (2004) Galectin-3 augments K-Ras activation and triggers a Ras signal that attenuates ERK but not phosphoinositide 3-kinase activity. *J Biol Chem* 279:34922–30

Elad-Sfadia G, Haklai R, Ballan E *et al.* (2002) Galectin-1 augments Ras activation and diverts Ras signals to Raf-1 at the expense of phosphoinositide 3-kinase. *J Biol Chem* 277:37169–75

Elola MT, Wolfenstein-Todel C, Troncoso MF *et al.* (2007) Galectins: matricellular glycan-binding proteins linking cell adhesion, migration, and survival. *Cell Mol Life Sci* 64:1679–700

Eude-Le Parco I, Gendronneau G, Dang T *et al.* (2009) Genetic assessment of the importance of galectin-3 in cancer initiation, progression, and dissemination in mice. *Glycobiology* 19:68–75

Freedman DA, Folkman J (2005) CDK2 translational down-regulation during endothelial senescence. *Exp Cell Res* 307:118–30

Fukumori T, Kanayama HO, Raz A (2007) The role of galectin-3 in cancer drug resistance. *Drug Resist Updat* 10:101–8

Gajewski TF (2007) Failure at the effector phase: immune barriers at the level of the melanoma tumor microenvironment. *Clin Cancer Res* 13:5256–61

Govindarajan B, Sligh JE, Vincent BJ *et al.* (2007) Overexpression of Akt converts radial growth melanoma to vertical growth melanoma. *J Clin Invest* 117:719–29

Greijer AE, van der Groep P, Kemming D *et al.* (2005) Up-regulation of gene expression by hypoxia is mediated predominantly by hypoxia-inducible factor 1 (HIF-1). *J Pathol* 206:291–304

Itahana K, Campisi J, Dimri GP (2007) Methods to detect biomarkers of cellular senescence: the senescence-associated beta-galactosidase assay. *Methods Mol Biol* 371:21–31

Krishnan V, Bane SM, Kawle PD *et al.* (2005) Altered melanoma cell surface glycosylation mediates organ specific adhesion and metastasis via lectin receptors on the lung vascular endothelium. *Clin Exp Metastasis* 22:11–24

La Porta CA (2009) Mechanism of drug sensitivity and resistance in melanoma. *Curr Cancer Drug Targets* 9:391–7

Le Mercier M, Lefranc F, Mijatovic T *et al.* (2008a) Evidence of galectin-1 involvement in glioma chemoresistance. *Toxicol Appl Pharmacol* 229:172–83

Le Mercier M, Mathieu V, Haibe-Kains B *et al.* (2008b) Knocking down galectin 1 in human hs683 glioblastoma cells impairs both angiogenesis and endoplasmic reticulum stress responses. *J Neuropathol Exp Neurol* 67:456–69

Le QT, Shi G, Cao H *et al.* (2005) Galectin-1: a link between tumor hypoxia and tumor immune privilege. *J Clin Oncol* 23:8932–41

Lim YC, Garcia-Cardena G, Allport JR *et al.* (2003) Heterogeneity of endothelial cells from different organ sites in T-cell subset recruitment. *Am J Pathol* 162:1591–601

Lin AW, Lowe SW (2001) Oncogenic ras activates the ARF-p53 pathway to suppress epithelial cell transformation. *Proc Natl Acad Sci USA* 98:5025–30

Liu FT, Rabinovich GA (2005) Galectins as modulators of tumour progression. *Nat Rev Cancer* 5:29–41

Liu FT, Rabinovich GA (2010) Galectins: regulators of acute and chronic inflammation. *Ann NY Acad Sci* 1183:158–82

Lotan R, Carralero D, Lotan D *et al.* (1989) Biochemical and immunological characterization of K-1735P melanoma galactoside-binding lectins and their modulation by differentiation inducers. *Cancer Res* 49:1261–8

Mathieu V, Le Mercier M, De Neve N *et al.* (2007) Galectin-1 knockdown increases sensitivity to temozolomide in a B16F10 mouse metastatic melanoma model. *J Invest Dermatol* 127:2399–410

Mansfield AS, Markovic SN (2009) Novel therapeutics for the treatment of metastatic melanoma. *Future Oncol* 5:543–57

Marneros AG (2009) Tumor angiogenesis in melanoma. *Hematol Oncol Clin North Am* 23:431–46

Mendelsohn R, Cheung P, Berger L *et al.* (2007) Complex N-glycan and metabolic control in tumor cells. *Cancer Res* 67:9771–80

Mouawad R, Spano JP, Khayat D (2010) Old and new serological biomarkers in melanoma: where we are in 2009. *Melanoma Res* 20:67–76

Nasrabadi D, Larijani MR, Fathi A *et al.* (2010) Nuclear proteome analysis of monkey embryonic stem cells during differentiation. *Stem Cell Rev* 6:50–61

Paz A, Haklai R, Elad-Sfadia G *et al.* (2001) Galectin-1 binds oncogenic H-Ras to mediate Ras membrane anchorage and cell transformation. *Oncogene* 20:7486–93

Platt D, Raz A (1992) Modulation of the lung colonization of B16-F1 melanoma cells by citrus pectin. *J Natl Cancer Inst* 84:438–42

Poirier F, Robertson EJ (1993) Normal development of mice carrying a null mutation in the gene encoding the L14 S-type lectin. *Development* 119:1229–36

Rubinstein N, Alvarez M, Zwirner NW *et al.* (2004) Targeted inhibition of galectin-1 gene expression in tumor cells results in heightened T cell-mediated rejection; A potential mechanism of tumor-immune privilege. *Cancer Cell* 5:241–51

Rye PD, Fodstad O, Emilsen E *et al.* (1998) Invasion potential and N-acetylgalactosamine expression in a human melanoma model. *Int J Cancer* 75:609–14

Schubbert S, Shannon K, Bollag G (2007) Hyperactive Ras in developmental disorders and cancer. *Nat Rev Cancer* 7:295–308. Erratum in: Nat Rev Cancer. 7:563

Serrano M, Lin AW, McCurrach ME *et al.* (1997) Oncogenic ras provokes premature cell senescence associated with accumulation of p53 and p16INK4a. *Cell* 88:593–602

Thijssen VL, Barkan B, Shoji H *et al.* (2010) Tumor cells secrete galectin-1 to enhance endothelial cell activity. *Cancer Res* 70:6216–24

Thijssen VL, Hulsmans S, Griffioen AW (2008) The galectin profile of the endothelium: altered expression and localization in activated and tumor endothelial cells. *Am J Pathol* 172:545–53

Thijssen VL, Postel R, Brandwijk RJ *et al.* (2006) Galectin-1 is essential in tumor angiogenesis and is a target for antiangiogenesis therapy. *Proc Natl Acad Sci USA* 103:15975–80

van den Brûle FA, Buicu C, Baldet M *et al.* (1995) Galectin-1 modulates human melanoma cell adhesion to laminin. *Biochem Biophys Res Commun* 209:760–7

Yaswen P, Campisi J (2007) Oncogene-induced senescence pathways weave an intricate tapestry. *Cell* 128:233–4

Zhuravliova E, Barbakadze T, Zaalishvili E *et al.* (2009) Social isolation in rats inhibits oxidative metabolism, decreases the content of mitochondrial K-Ras and activates mitochondrial hexokinase. *Behav Brain Res* 205: 377–83